Acta Crystallographica Section D
Biological Crystallography
ISSN 0907-4449

Structure of the transcription regulator CcpA from *Lactococcus lactis*

Bernhard Loll,[a]‡ Magdalena Kowalczyk,[b] Claudia Alings,[a] André Chieduch,[a] Jacek Bardowski,[b] Wolfram Saenger[a]* and Jacek Biesiadka[a]

[a]Institute for Chemistry and Biochemistry/ Crystallography, Freie Universität Berlin, Takustrasse 6, D-14195 Berlin, Germany, and [b]Department of Microbial Biochemistry, Institute of Biochemistry and Biophysics, PAS, Pawinskiego SA, 02-106 Warszawa, Poland

‡ Present address: Max-Planck Institute for Medical Research, Department of Biomolecular Mechanisms, Jahnstrasse 29, 69120 Heidelberg, Germany.

Correspondence e-mail: saenger@chemie.fu-berlin.de

Received 8 December 2006
Accepted 5 January 2007

PDB Reference: CcpA, 2o20, r2o20sf.

Catabolite control protein A (CcpA) functions as master transcriptional regulator of carbon catabolism in Firmicutes. It belongs to the family of bacterial repressor/regulator proteins. Here, the crystal structure of the 76 kDa homodimeric CcpA protein from *Lactococcus lactis* subsp. *lactis* IL1403 is presented at 1.9 Å resolution in the absence of cognate DNA. The phases were derived by molecular replacement and the structure was refined to crystallographic R and $R_{\rm free}$ factors of 0.177 and 0.211, respectively. The presence of a sulfate molecule in the direct vicinity of a putative effector-binding site in the monomer allowed the derivation of a model for the possible binding of small organic effector molecules.

1. Introduction

Carbon-catabolite repression is an important regulatory mechanism that permits bacteria to select and utilize a carbon source in order to provide the fastest growth rate (Stülke & Hillen, 2000). One of the global regulatory proteins for carbon-catabolite repression in Firmicutes is catabolite control protein A (CcpA; Henkin, 1996; Hueck *et al.*, 1995). CcpA binds to the conserved 14-nucleotide pseudo-palindromic DNA sequence *cre* (catabolite-responsive element; Miwa *et al.*, 2000; Weickert & Chambliss, 1989) and can thereby act either as an activator or repressor depending on the position of the *cre* site with respect to a given promoter sequence (Gösseringer *et al.*, 1997; Titgemeyer & Hillen, 2002).

The CcpA protein is a member of the GalR-LacI family of prokaryotic DNA-binding proteins that mainly regulate carbon, nitrogen and purine metabolism (Guédon *et al.*, 2002; Tobisch *et al.*, 1999). Crystal structures are available for two full-length GalR-LacI members bound to DNA: the purine repressor (PurR) and the lactose repressor (LacI) (Bell & Lewis, 2001; Lewis *et al.*, 1996; Schumacher *et al.*, 1994, 1995). Recently, exciting advances have been made in the understanding of how the different functional states of the CcpA protein are reflected at the structural level (Chaptal *et al.*, 2006; Schumacher *et al.*, 2004, 2006).

The proteins of the GalR-LacI family are composed of two domains: a 60-residue N-terminal DNA-binding domain comprising a helix–turn–helix (HTH) motif that is connected by a linker to a larger C-terminal domain of about 270 residues that resembles the fold of periplasmic binding proteins (PBPs; Fukami-Kobayashi *et al.*, 2003) and that can be further divided into N-terminal and C-terminal subdomains (PBP-N and PBP-C, respectively; Fig. 1).

Movement of the subdomains relative to each other leads to 'open' and 'closed' states of CcpA. In PurR and LacI proteins, the closed state facilitates optimal juxtaposition of the

attached hinge region of the DNA-binding domains, thereby permitting a structural change of the 'hinge' loop to a short helix associated with binding to cognate DNA. Interestingly, the DNA-bound states of PurR and LacI are structurally similar, yet in PurR the DNA-competent binding state is created by binding the co-repressor, either hypoxanthine or guanine, in the cavity between the PBP-N and PBP-C subdomains, while LacI is bound to DNA in the absence of effector (Bell & Lewis, 2001; Chaptal *et al.*, 2006; Lewis *et al.*, 1996; Schumacher *et al.*, 1994). Even though the DNA-bound states of GalR-LacI proteins are highly conserved in overall fold, their specific mechanisms of DNA binding differ. CcpA proteins diverge from other members of the GalR-LacI family as they are stimulated by phosphorylated proteins rather than by small organic effector molecules. The HPr protein, one of the key regulators of the phosphotransferase system of sugar uptake, can be phosphorylated at position Ser46. HPr-Ser46-P binds to CcpA, increasing the affinity of CcpA for DNA. It is still under debate whether small organic molecules such as NADP, glucose-6-phosphate (Glc-6-P) or fructose-1,6-bisphosphate (FBP) can have a similar effect on DNA binding (Gösseringer *et al.*, 1997; Kim *et al.*, 1998).

Lactococcus lactis belongs to the group of lactic acid bacteria. A great effort has been made to unravel the genetics and molecular biology of this microorganism. Many different bioengineering techniques have been optimized or developed for this bacterium and the genome of *L. lactis* was the first genome of the lactic acid bacteria to be sequenced (Bolotin *et al.*, 2001). *L. lactis* is commonly recognized as a model bacterium in studies on lactic acid bacteria and is one of the most frequently used microorganisms in the dairy industry, where it is used as a starter culture in many biotechnological processes, for example cheese production. Since the ability of *L. lactis* to ferment lactose to lactic acid, to degrade proteins and peptides and to produce diacetyl that is necessary for rapid acidification and the typical flavour of the dairy product, there is an interest in fully understanding the sugar metabolism and regulatory strategies of this Gram-positive bacterium.

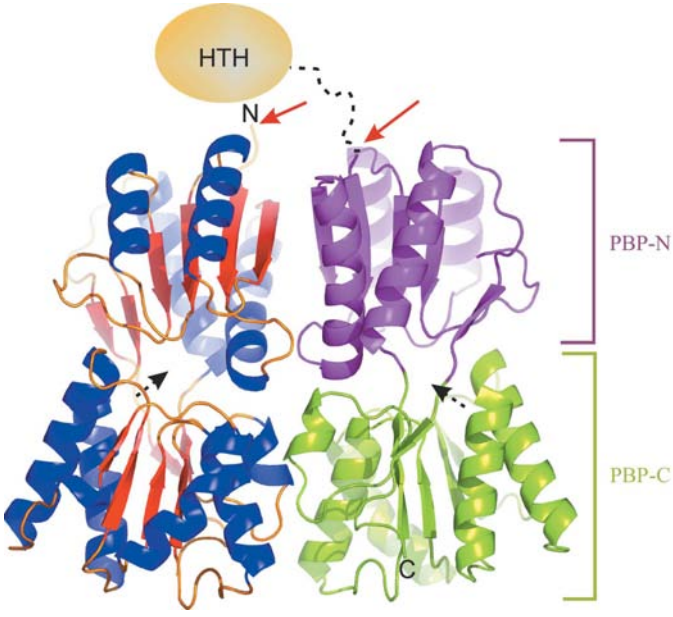

Figure 1
Ribbon representation of dimeric CcpA. The monomer on the left is coloured according to secondary-structure elements, with α-helices in blue, β-strands in red and loops in orange. The monomer on the right is coloured according to domain assignment, with the PBP-N subdomain in magenta and the PBP-C subdomain in green. For the monomer on the right, the N-terminal domain (light orange), comprising the HTH motif, and the linker region (black dashed line) are drawn schematically. Red arrows indicate the first modelled N-terminal domain of the CcpA monomers. Black arrows show the putative cofactor-binding site (see Fig. 2).

Table 1
Data-collection and refinement statistics.

Values in parentheses are for the highest resolution shell.

Data collection	
Wavelength (Å)	0.933
Temperature (K)	100.0
Space group	$P2_1$
Unit-cell parameters	a = 117.76, b = 74.27, c = 160.30, β = 102.36
Resolution (Å)	20.00–1.90 (1.95–1.90)
Unique reflections	211799 (15683)
Completeness (%)	99.4 (99.1)
$\langle I/\sigma(I)\rangle$	11.74 (4.49)
$R_{\rm meas}$†	0.104 (0.363)
Redundancy	5.5 (4.4)
Refinement	
No. of reflections used	201126
Reflections used for $R_{\rm free}$	10656
Non-H atoms	18486
Protein	17110
Chloride	1
Sulfate	40
Water	1332
$R_{\rm cryst}$‡	17.7 (22.5)
$R_{\rm free}$§	21.1 (27.6)
Overall B factor (Å^2)	29.7
Average B factors (Å^2)	
Protein	33.2
Chloride	20.7
Sulfates	40.8
Water	34.1
R.m.s.d. from ideal geometry¶	
Bond length (Å)	0.012
Bond angles (°)	1.289
Ramachandran plot††	
Core (%)	95.4
Allowed (%)	4.5
Generously allowed (%)	0.1

† $R_{\rm meas} = \sum_h [n/(n-1)]^{1/2} \sum_i |I_h - I_{h,i}| / \sum_h \sum_i I_{h,i}$, where I_h is the mean intensity of symmetry-equivalent reflections and n is the redundancy. ‡ $R_{\rm cryst} = \sum_h |F_{\rm o} - F_{\rm c}| / \sum F_{\rm o}$ (working set, no σ-cutoff applied). § $R_{\rm free}$ is the same as $R_{\rm cryst}$, but calculated on 5% of the data that were excluded from refinement. ¶ Root-mean-square deviation from target geometry. †† Calculated using *PROCHECK* (Laskowski *et al.*, 1993).

2. Materials and methods

2.1. Protein purification

For the purification of wild-type CcpA, the protocol described by Kowalczyk & Bardowski (2003) was applied with slight modifications. *Escherichia coli* BL21(DE3) cells harbouring a plasmid encoding the full-length CcpA protein of *L. lactis* subsp. *lactis* IL1403 with an N-terminal His_6 tag were used for the overexpression of CcpA. Centrifuged cells

were resuspended in buffer *A* (20 m*M* Tris–HCl pH 7.5, 500 m*M* NaCl, 10 m*M* imidazole) and disrupted using a French press. Cell debris was removed by centrifugation, the supernatant was loaded onto a HisTrap HP column (GE Healthcare) equilibrated with buffer *A* and the CcpA protein was eluted in a gradient of imidazole from 10 m*M* (buffer *A*) to 500 m*M* (buffer *B*; 20 m*M* Tris–HCl pH 7.5, 500 m*M* NaCl, 500 m*M* imidazole). The pooled fractions were concentrated using an Amicon Ultra-30 (Millipore) and loaded onto Superdex200 (GE Healthcare) equilibrated with buffer *C* (20 m*M* Tris–HCl pH 7.5, 500 m*M* NaCl). The protein eluted at 69 ml, corresponding to a molecular weight of about 76 kDa, indicating the presence of dimeric CcpA.

2.2. Mass spectrometry

Matrix-assisted laser desorption/ionization time-of-flight (MALDI–TOF) mass-spectrometry analysis was performed in the linear positive-ion mode with blanking ($m/z < 600$) and pulsed (time-delayed) extraction using a Shimadzu Biotech Axima TOF^2 instrument (Shimadzu Biotech Deutschland, Duisburg, Germany). All reagents and protein standards were from Sigma–Aldrich (Deisenhofen, Germany). Sinapinic acid [10 mg ml^{-1} in 50%(*v*/*v*) acetonitrile, 50%(*v*/*v*) 0.1% trifluoroacetic acid in water] was used as the matrix. The sample positions on the steel 384-position steel sample plate were washed once with matrix solution. With the help of a nylon loop, a frozen CcpA crystal was placed onto the sample plate and dissolved in 1 µl water. 1 µl matrix solution was mixed with the sample and the drop was allowed to dry at room temperature. Standard proteins (∼1 pmol of cytochrome *c*, myoglobin, aldolase or β-galactosidase in water) were spotted onto the washed plate and an equal volume (usually 1 µl) of matrix was immediately added to the protein drop. Each protein standard was analyzed separately and a combined calibration of the near external standards was employed to determine the mass/charge (*m*/*z*) values using the Shimadzu Biotech *Launchpad* v.2.7 software.

2.3. Protein crystallization and crystal cooling

Prior to crystallization, the protein was dialyzed against 20 m*M* Tris–HCl pH 7.5 and 300 m*M* NaCl. Crystallization screening experiments were performed using the sitting-drop vapour-diffusion method at 291 K in 96-well CrystalQuick plates (Greiner Bio-One, Germany). Initial conditions were refined and optimized in a hanging-drop vapour-diffusion setup in 24-well format. Crystals were obtained from drops made up of 1.5 µl protein solution (about 16 mg ml^{-1}) and 1.5 µl precipitant solution [22.5%(*w*/*v*) PEG 3350, 100 m*M* Li_2SO_4, 100 m*M* Tris–HCl pH 8.0] and grew within 3 d to dimensions of about 0.3 × 0.2 × 0.1 mm. Prior to cryocooling, the crystals were transferred to a reservoir solution complemented with 25%(*v*/*v*) glycerol as a cryoprotectant and were subsequently flash-cooled by plunging into liquid nitrogen.

2.4. Structure determination and refinement

A native X-ray diffraction data set was collected to 1.9 Å resolution at the European Synchrotron Radiation Facility (ESRF; Grenoble, France) on beamline ID 14-2 equipped with an ADSC Quantum CCD detector. The crystals belong to the monoclinic space group $P2_1$, with unit-cell parameters $a = 117.76$, $b = 74.27$, $c = 160.30$ Å, $\beta = 102.4^\circ$. X-ray data were processed and scaled with *XDS* (Kabsch, 1993) (Table 1). The structure of *L. lactis* CcpA was determined by molecular replacement using the program *PHASER* (Storoni *et al.*, 2004). All attempts to obtain phases for the CcpA protein by searching with various naturally occurring dimers were unsuccessful. Therefore, a search model was constructed from the PBP-N and PBP-C subdomains of truncated monomeric *Bacillus megaterium* CcpA protein (PDB code 1zvv, residues 61–332; Schumacher *et al.*, 2006). A subsequent search using monomeric CcpA resulted in an arrangement of eight monomers (four dimers) per asymmetric unit. A search using the DNA-binding domain failed. The molecular-replacement model was subjected to rigid-body refinement as implemented in the program *CNS* (Brünger *et al.*, 1998) to adjust the position of the PBP-N and PBP-C subdomains. Subsequent refinement steps included simulated annealing and refinement of grouped and individual atomic *B* factors. All these methods utilized the maximum-likelihood (MLF) target. Noncrystallographic symmetry restraints were strictly set for both molecular dynamics and positional refinement of simulated annealing.

Automatic model building was performed using *ARP*/*wARP* (Perrakis *et al.*, 1999) combined with iterative

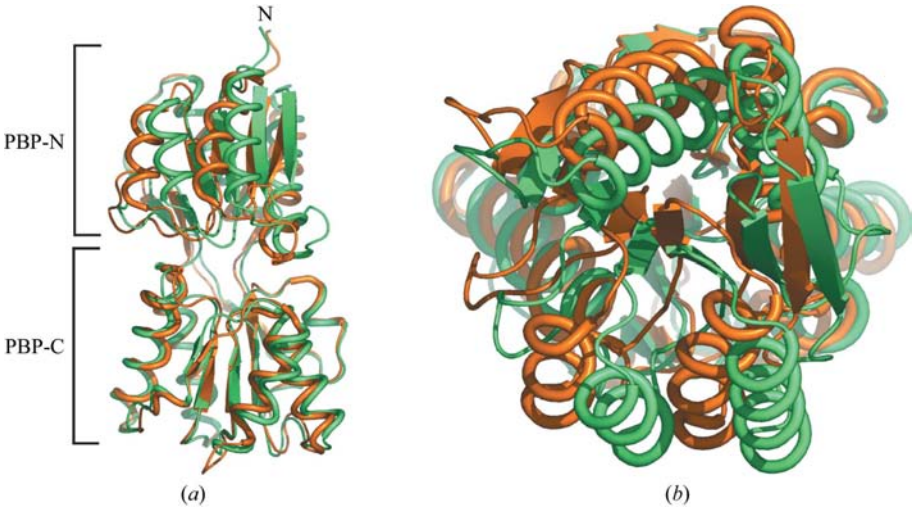

Figure 2
Superposition of *L. lactis* CcpA (green) and *B. megaterium* CcpA (orange; PDB code 1sxg) monomers using C^α atoms of the PBP-C subdomains. (*a*) Side view as in Fig. 1. (*b*) View rotated horizontally by 90°, with PBP-N at the front.

Table 2
Number of modelled residues and atoms per chain.

The overall *B* factor for each individual polypeptide chain is given.

Chain	Modelled residues	No. of protein atoms	Mean *B* factor (Å^2)
A	62–332	2135	24.0
B	58–332	2176	25.5
C	63–332	2106	54.6
D	63–332	2120	42.5
E	62–332	2153	20.0
F	61–332	2154	23.5
G	62–332	2116	32.3
H	61–332	2152	43.2

manual rebuilding using the program *O* (Jones *et al.*, 1991). In the final refinement steps, restrained maximum-likelihood refinement was executed using *REFMAC*5 (Murshudov *et al.*, 1999). At this stage, noncrystallographic symmetry restraints were not applied. Water molecules were positioned with *ARP*/*wARP* (Perrakis *et al.*, 1999) and fitted manually and their correct position was controlled using the program *Coot* (Emsley & Cowtan, 2004). For TLS refinement (Winn *et al.*, 2001), the PBP-N and PBP-C subdomains of each monomer were defined as separate TLS groups. Data-collection and selected refinement statistics are given in Table 1. Intermediate and final structures were evaluated with *PROCHECK* (Laskowski *et al.*, 1993) and *WHATCHECK* (Hooft *et al.*, 1996). The final model comprises 17 110 protein atoms, 1332 water molecules, eight sulfate molecules and one putative chloride anion. All figures were drawn using *PyMOL* (DeLano, 2002).

3. Results and discussion

3.1. Structural overview

CcpA from *L. lactis* was successfully overexpressed, purified and crystallized. This enabled us to determine the crystal structure to 1.9 Å resolution by molecular replacement and to refine it to crystallographic R and $R_{\rm free}$ factors of 0.177 and 0.211, respectively (Table 1). The crystallographic asymmetric unit contains four CcpA dimers with a Matthews coefficient (Matthews, 1968) of 2.2 Å^3 Da^{-1}, corresponding to a solvent content of 39%, assuming a molecular weight of about 38 kDa for the full-length protein with an N-terminal His_6 tag. Thus, the structure provides four independent views of dimeric CcpA that superimpose with a root-mean-square deviation (r.m.s.d.) of 0.6 Å for all equivalent CcpA C$^\alpha$ atoms. The eight monomeric subunits superimpose with an r.m.s.d. of 0.4 Å for all 268 equivalent pairs of CcpA C$^\alpha$ atoms. No significant differences were observed between the eight different monomers, except for differences in the number of modelled residues which originate from differences in the quality of the electron-density maps near the N-terminus of the PBP domain (Table 2). The average *B* factor differs slightly for the different monomers and dimers, respectively, owing to different crystal-packing contacts to symmetry-related protomers (Table 2).

The overall structure of *L. lactis* CcpA is similar to the fold of proteins belonging to the GalR-LacI family of bacterial transcription regulatory proteins. Characteristic of this fold are an N-terminal DNA-binding domain (residues 1–59) and a dimerization/co-repressor-binding domain (residues 60–332) composed of a PBP-N subdomain (residues 64–158 and 292–322) and a PBP-C subdomain (residues 164–293 and 324–332). The DNA-binding domain and the dimerization/co-repressor-binding domain are connected by a hinge region partly folded into a short α-helix.

The quality of the electron-density maps is excellent for the PBP domain and allowed tracing of all amino-acid residues. The PBP-N subdomain is composed of a central four-stranded parallel β-sheet sandwiched by four α-helices as well as an additional short two-stranded parallel β-sheet on the opposite side of the dimerization interface (see Fig. 1 and supplementary material[1]). The topography of the PBP-C subdomain is similar to that of the PBP-N subdomain and is composed of a central four-stranded parallel β-sheet surrounded by four α-helices, one short α-helix at the monomer–monomer interface and a short two-stranded antiparallel β-sheet as an extension of the central β-sheet that is oriented towards the solvent (see Fig. 1 and supplementary material[1]). The electron density around the N-terminal part of the PBP-N subdomain is fragmented and hence is uninterpretable. Proteolytic cleavage of CcpA during purification or crystallization can be excluded as MALDI–TOF mass spectrometry of the crystallized protein unequivocally revealed a molecular weight of 38 kDa corresponding to full-length protein with an N-terminal His_6 tag (spectra not shown). Further inspection of the crystal packing shows that there is sufficient space between the CcpA protomers to accommodate all undetectable N-terminal domains. Consequently, it must be disorder of this domain that prevents its localization in the electron density. A similar observation has been reported for the trehalose repressor of *E. coli*, a member of the LacI family (Hars *et al.*, 1998).

3.2. Comparison to *B. megaterium* CcpA structures

L. lactis CcpA shows 50.1% sequence identity and 76.4% similarity to the *B. megaterium* CcpA protein. According to the primary structure, the most conserved part is the DNA-binding domain, followed by the protein patches that are supposed to interact with the HPr protein. Monomeric *L. lactis* CcpA superimposes on the ternary CcpA–(HPr-Ser46-P)–*cre* complex or the truncated apo CcpA structure from *B. megaterium* with an r.m.s.d. of 1.7 Å for 270 pairs of C$^\alpha$ atoms (Fig. 2). However, an r.m.s.d. of 5.9 Å was calculated for 540 pairs of C$^\alpha$ atoms when the dimeric CcpAs were superimposed (see below for discussion).

The PBP-C subdomains of *L. lactis* and *B. megaterium* superimpose with an r.m.s.d. of 1.1 Å (136 pairs of C$^\alpha$ atoms) while the PBP-N subdomains differ more, with an r.m.s.d. of 1.5 Å (129 pairs of C$^\alpha$ atoms). In addition, a slight re-

[1] Supplementary material has been deposited in the IUCr electronic archive (Reference: WD5075). Services for accessing this material are described at the back of the journal.

orientation of the two domains is observed. These findings explain why no molecular-replacement solution was found by searching using CcpA dimers. A deletion in the primary sequence is found for a short loop region (around residue 240 according to *L. lactis* numbering) within the PBP-C subdomain. This deletion has no further influence on the overall structure of the protein or on the interaction with the HPr protein.

3.3. Monomer–monomer interface

The dimerization interface buries 1286 Å^2 per monomer of water-accessible surface compared with 1468 Å^2 in truncated CcpA or the CcpA–(HPr-Ser46-P)–*cre* complex as shown by the *PISA* server (Krissinel & Henrick, 2005). The dimerization interface is formed by residues 76–81 located on the first α-helix and second β-strand of the PBP-N subdomain as well as residues residing on two α-helices (248–260 and 278–282) of the PBP-C subdomain, respectively. A number of hydrogen bonds and salt bridges are formed across the monomer–monomer interface.

3.4. The HPr interface

The recently described interface between CcpA and HPr-Ser46-P of *B. megaterium* is exclusively formed by the PBP-N subdomain and HPr-Ser46-P (Schumacher *et al.*, 2004). Each of the PBP-N subdomains of dimeric CcpA interacts with one HPr-Ser46-P molecule. Based on superposition of our *L. lactis* structure with the *B. megaterium* CcpA in complex with HPr-Ser46-P, we modelled the structure of the complex formed by *L. lactis* HPr-Ser46-P protein and CcpA. The CcpA residues Tyr295, Ala299, Val300 and Leu304 (see supplementary material) are important for the interaction of the *L. lactis* proteins, as well as the HPr residues Ala16, Arg17, Gln24, Ile47, Met48 and Met51. Since all the latter residues are strictly conserved between *B. megaterium* and *L. lactis*, we conclude that the protein–protein interactions of CcpA and HPr-Ser46-P are structurally conserved between *B. megaterium* and *L. lactis*. Furthermore, the CcpA residues (Asp87, Arg303, Lys307; see supplementary material) which interact with the phosphorylated Ser46 are conserved in both organisms.

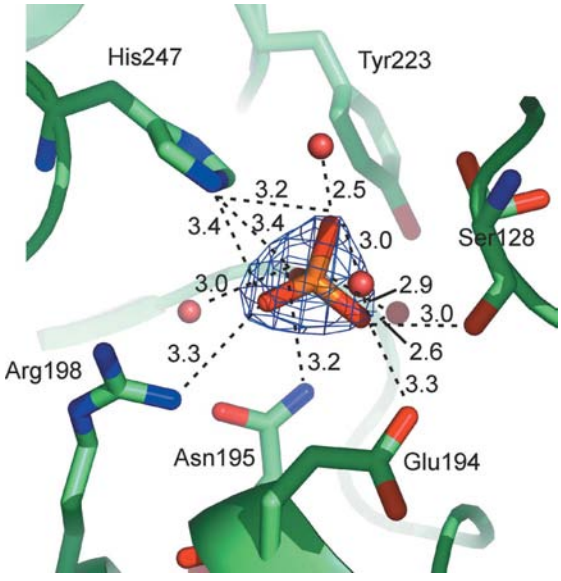

Figure 3
Putative cofactor-binding niche. CcpA is drawn in green. Sulfate-binding amino-acid side chains (green) and sulfate (orange) are shown in stick representation and surrounding water molecules within hydrogen-bonding distance are drawn as red spheres. Polar interactions within a distance of 3.4 Å are indicated by dashed black lines. Water molecules within a distance of less than 3.2 Å of the sulfate molecule are shown. The final $2F_o - F_c$ electron-density map (blue mesh) is contoured at 1σ and is limited to the sulfate molecule for clarity.

3.5. Putative effector-binding niche

Small organic molecules, such as the inducers for the GalR-LacI family, have been suggested as effectors for CcpA based on structure-based sequence alignments with LacI and GalR. A binding pocket has been suggested to be located in a cleft between the PBP-N and the PBP-C subdomains of the PBP domain (Fig. 1). Biochemical studies revealed that Glc-6-P or FBP enhance HPr-Ser46-P binding to CcpA (Deutscher *et al.*, 1995) and that FBP and NADP showed cooperative stimulation of CcpA binding to a 14-base-pair sequence at the start site of the α-amylase gene in the presence of HPr-Ser46-P (Kim *et al.*, 1998). Glc-6-P stimulated CcpA binding to *cre* in the absence of HPr-Ser46-P (Gösseringer *et al.*, 1997; Miwa *et al.*, 1997). Other studies showed that addition of Glu-6-P or FBP increased the affinity of HPr-Ser46-P for CcpA at least twofold and may therefore act as accessory co-repressors (Horstmann *et al.*, 2007; Seidel *et al.*, 2005). Interestingly, the ternary complex CcpA–(HPr-Ser46-P)–FBP shows the highest affinity for DNA, with a K_d of 90 μM (Kim *et al.*, 1998).

DALI superposition (Holm & Sander, 1993) of the tertiary structure of CcpA of *L. lactis* revealed the expected high similarity to the structures of *B. megaterium* CcpA protein (PDB code 2sxg; *Z* score 36.0) as well as LacI (PDB code 1qpz; *Z* score 32.0). The next highest scores all belong to periplasmic proteins that act as primary receptors for chemotaxis and transport: for instance, D-ribose-binding protein complexed with ribose (PDB code 2dri; *Z* score 29.6) and L-arabinose-binding protein (PDB code 8abp; *Z* score 25.1).

The electron density showed a sulfate molecule originating from the crystallization buffer in a niche that is close to the cleft between the PBP-N and PBP-C subdomains of one protomer (Fig. 3). This niche was suggested to be a putative binding pocket for small organic effector molecules. The location is remarkable as the sulfate might mimic the phosphate function of Glc-6-P or FBP. The sulfate interacts directly with the side chains of Ser128 O, Glu194 OE2, Asn195 ND2, Arg198 NH1 and His247 NE1 and indirectly *via* water molecules with Ser189 N, Tyr223 OH and Ser246 OG. Examination of the structure of CcpA–HPr-Ser46-P bound to *cre* showed that the binding pocket for putative effectors would even be accessible in the presence of HPr-Ser46-P.

Crystallization trials in presence of 10 m*M* Glc-6-P were performed under the same crystallization conditions as for CcpA. So far, these experiments have not been successful, which might provide hints of a possible rearrangement of amino-acid side chains or even domain rearrangements upon binding of the cofactor.

The authors are grateful to Deutsche Forschungsgemeinschaft for support in the frame of Sonderforschungsbereich 498 (to BL and JB), to Fonds der Chemischen Industrie (to WS) and to the Max-Planck Gesellschaft (to BL). This work was supported by grant No. 2 P04B02528 from the Polish Ministry of Education and Science. Beam time and support at the ESRF (Grenoble; France) is gratefully acknowledged. Thanks are expressed to Robert Shoeman for recording MALDI–TOF mass-spectrometry spectra.

References

Bell, C. E. & Lewis, M. (2001). *Curr. Opin. Struct. Biol.* **11**, 19–25.
Bolotin, A., Wincker, P., Mauger, S., Jaillon, O., Malarme, K., Weissenbach, J., Ehrlich, S. D. & Sorokin, A. (2001). *Genome Res.* **11**, 731–753.
Brünger, A. T., Adams, P. D., Clore, G. M., DeLano, W. L., Gros, P., Grosse-Kunstleve, R. W., Jiang, J.-S., Kuszewski, J., Nilges, M., Pannu, N. S., Read, R. J., Rice, L. M., Simonson, T. & Warren, G. L. (1998). *Acta Cryst.* D**54**, 905–921.
Chaptal, V., Gueguen-Chaignon, V., Poncet, S., Lecampion, C., Meyer, P., Deutscher, J., Galinier, A., Nessler, S. & Morera, S. (2006). *Proteins*, **64**, 814–816.
DeLano, W. L. (2002). *The PyMOL Molecular Graphics System.* http://www.pymol.org.
Deutscher, J., Kuster, E., Bergstedt, U., Charrier, V. & Hillen, W. (1995). *Mol. Microbiol.* **15**, 1049–1053.
Emsley, P. & Cowtan, K. (2004). *Acta Cryst.* D**60**, 2126–2132.
Fukami-Kobayashi, K., Tateno, Y. & Nishikawa, K. (2003). *Mol. Biol. Evol.* **20**, 267–277.
Gösseringer, R., Küster, E., Galinier, A., Deutscher, J. & Hillen, W. (1997). *J. Mol. Biol.* **266**, 665–676.
Guédon, E., Jamet, E. & Renault, P. (2002). *Antonie van Leeuwenhoek*, **82**, 93–112.
Hars, U., Horlacher, R., Boos, W., Welte, W. & Diederichs, K. (1998). *Protein Sci.* **7**, 2511–2521.
Henkin, T. M. (1996). *FEMS Microbiol. Lett.* **135**, 9–15.
Holm, L. & Sander, C. (1993). *J. Mol. Biol.* **233**, 123–138.
Hooft, R. W., Vriend, G., Sander, C. & Abola, E. E. (1996). *Nature (London)*, **381**, 272.
Horstmann, N., Seidel, G., Aung-Hilbrich, L.-M. & Hillen, W. (2007). *J. Biol. Chem.* **282**, 1175–1182.
Hueck, C. J., Kraus, A., Schmiedel, D. & Hillen, W. (1995). *Mol. Microbiol.* **16**, 855–864.
Jones, T. A., Zou, J.-Y., Cowan, S. W. & Kjeldgaard, M. (1991). *Acta Cryst.* A**47**, 110–119.
Kabsch, W. (1993). *J. Appl. Cryst.* **26**, 795–800.
Kim, J. H., Voskuil, M. I. & Chambliss, G. H. (1998). *Proc. Natl Acad. Sci. USA*, **95**, 9590–9595.
Kowalczyk, M. & Bardowski, J. (2003). *Acta Biochim. Pol.* **50**, 455–459.
Krissinel, E. & Henrick, K. (2005). *Detection of Protein Assemblies in Crystals.* Berlin: Springer-Verlag.
Laskowski, R. A., MacArthur, M. W., Moss, D. S. & Thornton, J. M. (1993). *J. Appl. Cryst.* **26**, 283–291.
Lewis, M., Chang, G., Horton, N. C., Kercher, M. A., Pace, H. C., Schumacher, M. A., Brennan, R. G. & Lu, P. (1996). *Science*, **271**, 1247–1254.
Matthews, B. W. (1968). *J. Mol. Biol.* **33**, 491–497.
Miwa, Y., Nagura, K., Eguchi, S., Fukuda, H., Deutscher, J. & Fujita, Y. (1997). *Mol. Microbiol.* **23**, 1203–1213.
Miwa, Y., Nakata, A., Ogiwara, A., Yamamoto, M. & Fujita, Y. (2000). *Nucleic Acids Res.* **28**, 1206–1210.
Murshudov, G. N., Vagin, A. A., Lebedev, A., Wilson, K. S. & Dodson, E. J. (1999). *Acta Cryst.* D**55**, 247–255.
Perrakis, A., Morris, R. & Lamzin, V. S. (1999). *Nature Struct. Biol.* **6**, 458–463.
Schumacher, M. A., Allen, G. S., Diel, M., Seidel, G., Hillen, W. & Brennan, R. G. (2004). *Cell*, **118**, 731–741.
Schumacher, M. A., Choi, K. Y., Lu, F., Zalkin, H. & Brennan, R. G. (1995). *Cell*, **83**, 147–155.
Schumacher, M. A., Choi, K. Y., Zalkin, H. & Brennan, R. G. (1994). *Science*, **266**, 763–770.
Schumacher, M. A., Seidel, G., Hillen, W. & Brennan, R. G. (2006). *J. Biol. Chem.* **281**, 6793–6800.
Seidel, G., Diel, M., Fuchsbauer, N. & Hillen, W. (2005). *FEBS Lett.* **272**, 2566–2577.
Storoni, L. C., McCoy, A. J. & Read, R. J. (2004). *Acta Cryst.* D**60**, 432–438.
Stülke, J. & Hillen, W. (2000). *Annu. Rev. Microbiol.* **54**, 849–880.
Titgemeyer, F. & Hillen, W. (2002). *Antonie Van Leeuwenhoek*, **82**, 59–71.
Tobisch, S., Zuhlke, D., Bernhardt, J., Stülke, J. & Hecker, M. (1999). *J. Bacteriol.* **181**, 6996–7004.
Weickert, M. J. & Chambliss, G. H. (1989). *J. Bacteriol.* **171**, 3656–3666.
Winn, M. D., Isupov, M. N. & Murshudov, G. N. (2001). *Acta Cryst.* D**57**, 122–133.